Available online at www.sciencedirect.com
SCIENCE DIRECT®
Chemical Physics Letters 408 (2005) 107–111
CHEMICAL PHYSICS LETTERS
www.elsevier.com/locate/cplett

High temperature rate coefficient measurements of H + O_2 chain-branching and chain-terminating reaction

S.M. Hwang [a], Si-Ok Ryu [b], K.J. De Witt [a], M.J. Rabinowitz [c,*]

[a] Department of Chemical Engineering, University of Toledo, Toledo, OH 43606, United States
[b] Department of Chemical Engineering, Yeungnam University, Dae Gu, South Korea
[c] NASA, Glenn Research Center at Lewis Field, Research and Technology Directorate, Mail Stop 5-10, Brook Park, OH 44135-3191, United States

Received 15 March 2005; in final form 30 March 2005
Available online 26 April 2005

Abstract

Rate coefficients for $H + O_2 \rightarrow OH + O$ (R_1) and $H + O_2 + M \rightarrow HO_2 + M$ (R_9) were measured via OH absorption behind reflected shock waves, being: $k_1 = 6.73 \times 10^{15}\, T^{-0.50}\, \exp(-8390\ \mathrm{K}/T)\ \mathrm{cm^3\,mol^{-1}\,s^{-1}}$ at $T = 950$–3100 K and $k_{9,0}/[\mathrm{Ar}] = 5.55 \times 10^{18}\, T^{-1.15}\ \mathrm{cm^6\,mol^{-2}\,s^{-1}}$ at $T = 950$–1200 K. Our experimental results for k_1 strongly support recent ab initio calculations showing temperature curvature due to back dissociation, $HO_2 \rightarrow O + OH$ following $O + OH \rightarrow HO_2$ if the reaction is considered from the reverse direction.
Published by Elsevier B.V.

1. Introduction

The overall reaction $H + O_2 \rightarrow$ products has been intensively studied due to both its practical and theoretical importance. Nearly, all reaction characteristics (flame speeds, ignition behavior, extinction, etc.) in hydrogen and hydrocarbon combustion are controlled by the balance between chain-branching and chain-termination in the overall reaction. Theoretically, understanding the delicate interplay between complex stability, energy barriers and entrance/exit channels for the overall reaction has remained a major challenge. The extent of back reaction and the relative contributions from statistical and non-statistical processes, and thus curvature in the rate expression, has been extensively debated. Experimental studies have also been inconsistent as to the extent or existence of curvature. Historically, three sources of data have been used to develop the reaction mechanism for H_2/O_2 system: static bulb measurements of the three explosion limits of stoichiometric H_2/O_2 mixtures at $T = 670$–840 K [1], shock tube measurements of diluted H_2/O_2 mixtures at higher temperatures and densities [2], and high temperature flow tube experiments [3]. Over fifty years of experimental and theoretical studies have been performed to obtain the rate coefficients of R_1 ($H + O_2 \rightarrow OH + O$) and R_9 ($H + O_2 + M \rightarrow HO_2 + M$); although steady progress has been made, significant disagreement still exists in their determination.

For R_1, the primary obstacle has been the difficulty in performing experiments at relatively low temperatures. This has prohibited any single group from obtaining consistent results over a sufficiently wide temperature range. Instead, many groups have added Pirraglia et al.'s [4] low temperature k_1 values ($T = 960$–1200 K) to their own high temperature measurements in order to develop k_1 expressions that cover the range of importance to combustion applications (some groups have used Semenov's evaluation [5] below 800 K, see references therein). This

* Corresponding author. Fax: +1 216 433 5802.
E-mail address: martin.j.rabinowitz@nasa.gov (M.J. Rabinowitz).

0009-2614/$ - see front matter. Published by Elsevier B.V.
doi:10.1016/j.cplett.2005.03.140

work is the first by a single group covering the entire range of interest above 950 K. Considering the importance of R_1, the discrepancies among the results are still large, a factor of 1.3 at 1050 K [4,6]. For R_9, although a consensus rate coefficient value has been established at room temperature [7], the scatter of the data is also quite large at $T > 750$ K – a factor of 3 at $T = 1000$ K (see Fig. 3b).

2. Experimental conditions and computer simulation

The experimental apparatus, operation and temperature correction methodology are described in detail elsewhere [6,8]. $H_2/O_2/Ar$ mixtures were prepared manometrically and allowed to stand for at least 48 h before use. Gases were used as delivered: H_2, 99.9995% (MG Industries, Scientific Grade); O_2, 99.999% (MG Industries, Scientific Grade); and, Ar, 99.9999% (MG Industries, UHP Grade).

Our trial reaction mechanism is based upon our previous H_2/O_2 mechanism [6] with the following revisions: k_2 ($O + H_2 \rightarrow OH + H$) from Sutherland et al. [9]; k_{10} ($HO_2 + H \rightarrow OH + OH$) from GRI 3.0 [G.P. Smith, et al., GRI-Mech, http://www.me.berkeley.edu/gri_mech/]; k_{15}($HO_2 + HO_2 \rightarrow H_2O_2 + O_2$) and k_{20}($H_2O_2 + OH \rightarrow H_2O + HO_2$) from Baulch et al. [7] NASA thermodata [10], employing the recent OH bond dissociation energy of $D^0_{298.15}(HOH) = 118.81 \pm 0.07$ kcal mol^{-1} [11], has been used throughout this study. Post reflected shock conditions were corrected for boundary layer/reflected shock interaction using the methodology described in Hwang et al. [8]. As we have previously demonstrated [6,8,12], the effect of O_2 vibrational relaxation time on our rate coefficient measurement was insignificant.

An extensive sensitivity study, using profile parameterization, was performed to select optimal experimental conditions. For the low temperature k_1 determination, the parameter chosen was $NS_m = \max(-[dI/I_0]/dt)/A_m$, where $A_m = (1 - I/I_0)_{max}$ (see figure 3 of [6]). A series of mixture compositions, given by percent H_2 and equivalence ratio (ϕ), was selected, namely: 1.0% H_2, $\phi = 1.0$; 10.0% H_2, $\phi = 2.5$; 6.0% H_2, $\phi = 3.0$; 15.0% H_2, $\phi = 3.0$. For the determination of R_9, the parameters chosen were τ_{75} (time to reach 75% of A_m) and NS_m. As expected, the sensitivity of R_9 increases with increasing ρ and with decreasing ϕ and T; thus, very lean mixtures were chosen: 0.5% H_2, $\phi = 0.025$; 0.25% H_2, $\phi = 0.025$; 0.25% H_2, $\phi = 0.0125$. The experiments were designed to vary ρ (×2 or ×3) in the same mixture composition (0.25% H_2, $\phi = 0.0125$) or to vary ρ by a factor of ~2, while keeping the initial aftershock [H_2] and [O_2] constant in the $\phi = 0.025$ mixtures. Extreme time scale and absorption level for our apparatus and sensitivities restricted our T-ranges to $T = 950$–3100 K for R_1 and 950–1200 K for R_9.

3. Results

The rate coefficients of R_1 and R_9 were obtained via direct computer simulations of experimental absorption profiles (not parameterizations as used in the sensitivity analysis). For R_1, 360 profiles were used (including the previous high temperature results of eight rich mixtures [6]) and for R_9, 118 profiles were used. In the simulation, only the rate coefficient of either R_1 or R_9 was varied. The matches between experimental and simulated pre-peak absorption profiles were excellent over the full range of T and ϕ. Post-peak profile matching, while good, could be improved by varying k_3 ($OH + H_2 \rightarrow H_2O + H$) for R_1 and k_{14} ($OH + HO_2 \rightarrow H_2O + O_2$) for R_9. Nevertheless, the resultant changes in k_1 or $k_{9,0}$/[Ar] were insignificant.

Typical experimental and simulated absorption profiles are shown in Fig. 1 and the resultant k_1 values and their deviations from the least squares fit expression are plotted in Fig. 2a,b. The least squares fit to the data gives,

$$k_1 = 6.73 \times 10^{15}\ T^{-0.50} \exp(-8390\ \mathrm{K}/T)\ \mathrm{cm^3\ mol^{-1}\ s^{-1}},$$

for $T = 950$–3100 K with $\sigma = \pm 7\%$.

For R_9, we determined the collision–efficiency-corrected $k_{9,0}$/[M] values for M = Ar; i.e., optimized $k_{9,0}$ values were scaled with $[M] = \rho \times [1 + x(O_2)(\varepsilon(O_2) - 1) + x(H_2)(\varepsilon(H_2) - 1) + x(H_2O)(\varepsilon(H_2O) - 1)]$, where the collision efficiencies are: $\varepsilon(H_2O) = 21.3$, $\varepsilon(H_2) = 3.33$, $\varepsilon(O_2) = 1.33$, and ε (other species including Ar) = 1.0. Because of the rather narrow temperature range of this

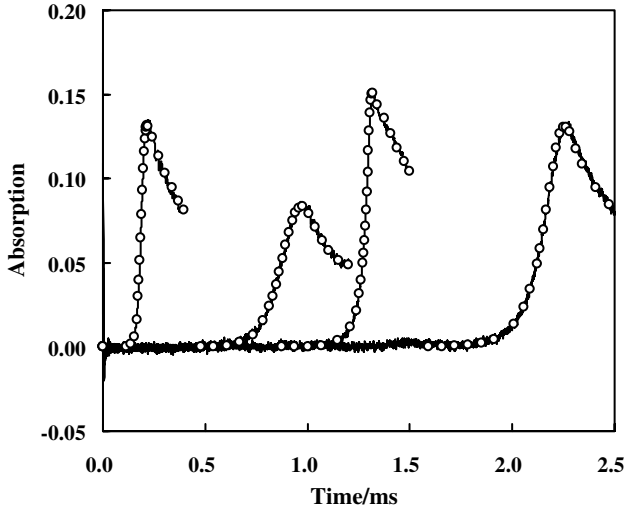

Fig. 1. Experimental (black solid) and simulated (open circles) OH absorption profiles. Profiles from the left are: 4% H_2, $\phi = 2.0$, 1243 K, 2.46 atm, $\tau_m = 0.22$ ms, $A = A_{actual}/5$; 5% H_2, $\phi = 5.0$, 1243 K, 0.80 atm, $\tau_m = 0.97$ ms, $A = A_{actual}$; 15% H_2, $\phi = 3.0$, 999 K, 1.11 atm, $\tau_m = 1.32$ ms, $A = A_{actual}/4$; 4% H_2, $\phi = 2.0$, 999 K, 1.53 atm, $\tau_m = 2.27$ ms, $A = A_{actual}/2$.

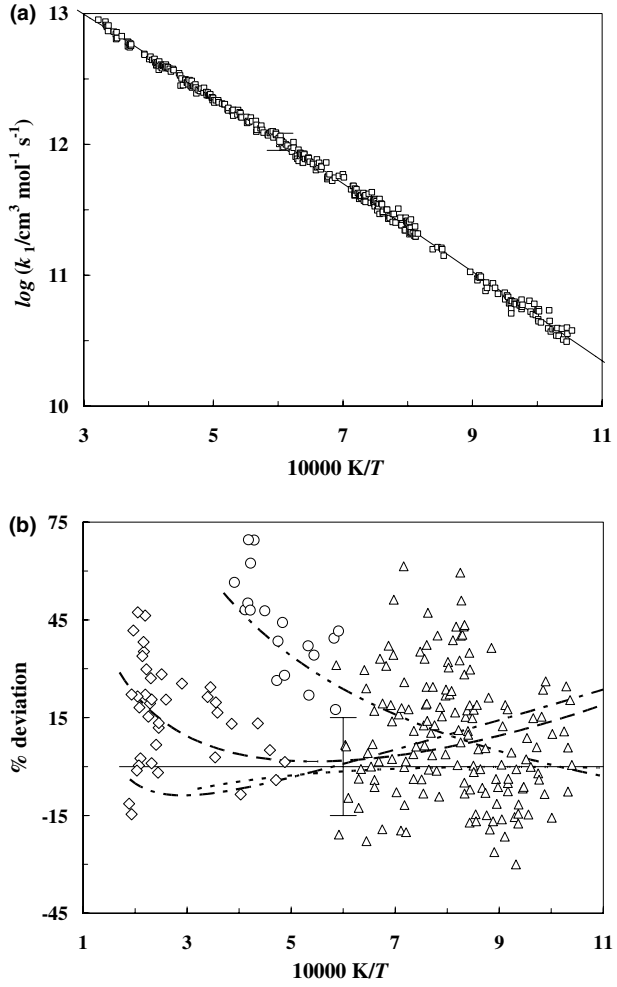

Fig. 2. (a) Non-Arrhenius plot of the experimental data for k_1. The solid line is the least squares fit to the data. The error bars represent ±15% of the propagation uncertainty limit of the individual measurements. (b) Comparison of the selected k_1 values and expressions with our expression. %Deviation = $(k_{1,\text{others}}-1)\times 100/k_{1,\text{this study}}$. Symbols and references are: open circle, [14]; open triangle, [4]; open diamond, [13]. Lines and references are: dot dot dash, [4]; long dash, [7] and [13]; dash, [GRI 3.0, G.P. Smith, et al., GRI-Mech, http://www.me.berkeley.edu/gri-mech/]; dot dash, [17]; solid, (this study).

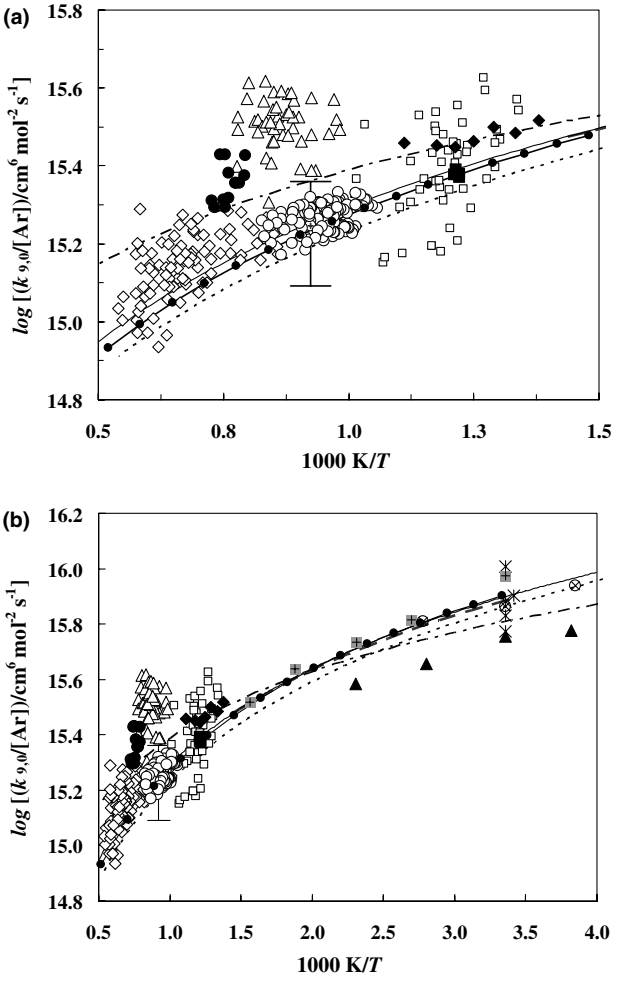

Fig. 3. (a) Comparison of $k_{9,0}$/[Ar] at $T > 667$ K. Symbols and references are: open diamond, [20]; open triangle up, [18]; open square, [4]; filled circle, [19]; filled diamond, [21]; filled square, [22]; open circle, (this study). Lines are: dot dash, [7]; dash, [23]; gray long dash, [24]; filled circle on solid line, [25]. The error bars represent ±30% of our $k_{9,0}$/[Ar]. (b) Comparison of $k_{9,0}$/[Ar] at entire temperature range. Lines and symbols are as in Fig. 3a. Additional symbols and references are: filled triangle, [26]; open circle with '×' inside, [27]; gray filled square with '+' inside, [28]; star, room – T data (see table 3 in 24).

study, we included the previously reported low temperature data ($T < 990$ K) for the fit (see Fig. 3a,b). A power law expression, $k_{9,0}$/[Ar] = $AT^n\exp(-\Theta/T)$ with $\Theta = 0$ K yields

$$k_{9,0}/[\text{Ar}] = 5.55\times 10^{18}\ T^{-1.15}\ \text{cm}^6\ \text{mol}^{-2}\ \text{s}^{-1},$$

for $T = 950$–1200 K and $[\text{Ar}] = 15 - 53$ μmol cm^{-3}.

Propagation-of-error analyses were performed for k_1 and $k_{9,0}$/[Ar] using uncertainty contributions from the transducers, mixture composition, shock velocity, P_5 (used in the temperature correction) and cross-coupling of other reactions in the computer simulation. The maximum uncertainties calculated using the formula $U = (\Sigma U_i^2)^{1/2}$, are ±15% for k_1 and ±30% for $k_{9,0}$/[Ar].

4. Discussion

We examined the effect of flow disturbance by either boundary layer interactions or contact surface or rarefaction wave arrival. Fig. 1 shows the experimental and simulated absorption profiles for experiments at two temperatures, but having very different time to peak absorption for each temperature. For a corrected temperature of 1243 K (left two), the peak absorptions occurred at 0.22 and 0.97 ms, while for a corrected temperature of 999 K (right two) the peak absorptions occurred at 1.32 and 2.27 ms. The k_1 values from the same corrected temperature (average temperature corrections are 1.4%) are in agreement within the uncertainty limits. The observed peak absorption for a 10.0% H_2, $\phi = 2.5$ mixture at $T = 961$ K occurred at

2.30 ms while the calculated contact surface arrival time was 2.85 ms. Rarefaction waves never crossed contact surface.

4.1. Chain-branching R_1 ($H + O_2 \rightarrow OH + O$)

Many k_1 expressions are currently used ($cm^3\,mol^{-1}\,s^{-1}$): Pirraglia et al. [4] (962–2577 K), $1.92 \times 10^{14}\,\exp(-8272\,K/T)$; Du and Hessler [13] (960–5300 K), and Baulch et al. [7] (300–5300 K), $9.76 \times 10^{13}\,\exp(-7474\,K/T)$; GRI 3.0 (300–3000 K), $2.65 \times 10^{16}\,T^{-0.6707}\,\exp(-8575\,K/T)$. These expressions are fits to the combined results of many individual studies using different temperature ranges, compositions, diagnostics and optimization schemes.

As shown in Fig. 2a,b, our rate coefficients are in good agreement with the Pirraglia et al. experimental results (low temperatures), but not with the overall fit (high temperatures are from the data of Frank and Just [14]). In the range 950–2500 K, we are in good agreement with the expressions of Baulch et al., Du and Hessler and the GRI 3.0 optimization. Above 2500 K, the absolute values of Du and Hessler and this study are in within the combined error limits, but our T-dependence of −0.50 separates from their non-T-dependent expression.

Three notable theoretical calculations for R_1 are that of Miller [15], Varandas et al. [16], and Troe and Ushakov [17]. Briefly, Miller obtains a negative curvature of −0.816 due to dynamical effects involving the light H-atom and Varandas et al. see no curvature of the rate coefficient expression derived from calculations using their DMBE IV potential energy surface. Detailed reviews for these two works are given in [6,17]. Recently, Troe and Ushakov performed classical trajectory calculations for R_{-1} ($O + OH \rightarrow H + O_2$) using their new potential energy surface (based upon the high precision ab initio calculation along the MEP of $HO_2 \rightarrow H + O_2$ and $HO_2 \rightarrow O + OH$) that revealed the importance of the both statistical and non-statistical back dissociation, $HO_2 \rightarrow O + OH$ following $O + OH \rightarrow HO_2$ at $T > 500$ K (considered from the reverse direction). This back reaction leads to a negative T-dependence of −0.465 (derived from fitting their k_{-1} values and our K_{eq}), in good agreement with our measured value of −0.50.

4.2. Chain-terminating R_9 ($H + O_2 + M \rightarrow HO_2 + M$)

Shown in Fig. 3a,b are our $k_{9,0}$/[Ar] values plotted along with those of selected previous studies. The values of Gutman et al. [18] and Davidson et al. (calculated from their falloff data) [19] are higher than ours and outside of our upper uncertainty limit (+30%). At high temperatures, the majority of Getzinger and Schott's data [20] are somewhat higher than our values. At low temperatures, our extrapolated values have a general agreement with the results of Pirraglia et al. [4] and Ashman and Haynes [21]. There is particularly good agreement between our values and those of Mueller et al. [22]. Also displayed in Fig. 3a,b are the rate coefficient expressions of Baulch et al. [7], Bates et al. [23], Michael et al. [24] and Troe [25]. As seen, the extrapolation from the expression of Michael et al. for M = Ar ($4.57 \times 10^{18}\,T^{-1.12}\,cm^6\,mol^{-2}\,s^{-1}$, $T = 296$–700 K) represents our data equally well.

5. Conclusions

We present a consistent set of rate data in the wide temperature range ($T = 950$–3100 K) for the chain-branching reaction R_1 ($H + O_2 \rightarrow OH + O$). Our rate coefficient measurements at low temperatures ($T < 1200$ K) agree well with those of Pirraglia et al. [4] and with the GRI expression over our entire temperature range. Our data supports the negative temperature coefficient of Troe and Ushakov [17] and is well represented by the following non-Arrhenius expression:

$$k_1 = 6.73 \times 10^{15}\,T^{-0.50}\exp(-8390\,K/T)\ cm^3\ mol^{-1}\ s^{-1}$$

for $T = 950$–3100 K with propagated uncertainty limits of ±15%.

Our low pressure limit rate coefficients of the chain-terminating reaction R_9 ($H + O_2 + M \rightarrow HO_2 + M$) are in the lower range of previous results. A power law expression derived using the combined data of this work and the previous low temperature studies gives:

$$k_{9,0}/[Ar] = 5.55 \times 10^{18}\,T^{-1.15}\ cm^6\ mol^{-2}\ s^{-1}$$

for $T = 950$–1200 K and [Ar] = 15–53 μmol cm^{-3} with propagated uncertainty limits of ±30%.

References

[1] G. Dixon-Lewis, D.J. Williams, in: C.H. Bamford, C.F.H. Tipper (Eds.), Comprehensive Chemical Kinetics, vol. 17, Elsevier, New York, 1977, p. 1.
[2] J.W. Meyer, A.K. Oppenheim, Proc. Combust. Inst. 13 (1971) 1153.
[3] M.A. Mueller, T.J. Kim, R.A. Yetter, F.L. Dryer, Int. J. Chem. Kinet. 31 (1999) 113.
[4] A.N. Pirraglia, J.V. Michael, J.W. Sutherland, R.B. Klemm, J. Phys. Chem. 93 (1989) 282.
[5] N. Semenov, Acta Physicochim. U.R.S.S. 20 (1945) 291.
[6] S.-O. Ryu, S.M. Hwang, M.J. Rabinowitz, J. Phys. Chem. 99 (1995) 13984.
[7] D.L. Baulch, C.J. Cobos, R.A. Cox, P. Frank, G. Hayman, Th. Just, J.A. Kerr, T. Murrells, M.J. Pilling, J. Troe, R.W. Walker, J. Warnatz, J. Phys. Chem. Ref. Data 23 (1994) 847.
[8] S.M. Hwang, S.-O. Ryu, K.J. De Witt, M.J. Rabinowitz, J. Phys. Chem. 103 (1999) 5949.

[9] J.W. Sutherland, J.V. Michael, A.N. Pirraglia, F.L. Nesbitt, R.B. Klemm, Proc. Combust. Inst. 21 (1986) 929.
[10] B.J. McBride, M.J. Zehe, S. Gordon, NASA Glenn Coefficients for Calculating Thermodynamic Properties of Individual Species, NASA/TP–2002-211556, NASA, Washington, DC, 2002.
[11] B. Ruscic, A.F. Wagner, L.B. Harding, R.L. Asher, D. Feller, D.A. Dixon, K.A. Peterson, Y. Song, X. Qian, C.-Y. Ng, J. Liu, W. Chen, D.W. Schwenke, J. Phys. Chem. A 106 (2002) 2727.
[12] R.C. Millikan, R.R. White, J. Chem. Phys. 39 (1963) 3209.
[13] H. Du, J.P. Hessler, J. Chem. Phys. 96 (1992) 1077.
[14] P. Frank, Th. Just, Ber. Bunsen. Phys. Chem. 89 (1985) 181.
[15] J.A. Miller, J. Chem. Phys. 84 (1986) 6170.
[16] A.J.C. Varandas, J. Brandão, M.R. Pastrana, J. Chem. Phys. 96 (1992) 5137.
[17] J. Troe, V.G. Ushakov, J. Chem. Phys. 115 (2001) 3621.
[18] D. Gutman, E.A. Hardwidge, F.A. Dougherty, R.W. Lutz, J. Chem. Phys. 47 (1967) 5950.
[19] D.F. Davidson, E.L. Petersen, M. Röhrig, R.K. Hanson, C.T. Bowman, Proc. Combust. Inst. 26 (1996) 481.
[20] R.W. Getzinger, G.L. Schott, J. Chem. Phys. 43 (1965) 3237.
[21] P.J. Ashman, B.S. Haynes, Proc. Combust. Inst. 27 (1998) 185.
[22] M.A. Mueller, R.A. Yetter, F.L. Dryer, Proc. Combust. Inst. 27 (1998) 177.
[23] R.W. Bates, D.M. Golden, R.K. Hanson, C.T. Bowman, Phys. Chem. Chem. Phys. 3 (2001) 2337.
[24] J.V. Michael, M.-C. Su, J.W. Sutherland, J.J. Caroll, A.F. Wagner, J. Phys. Chem. A 106 (2002) 5297.
[25] J. Troe, Proc. Combust. Inst. 28 (2000) 1463.
[26] M.J. Kurylo, J. Phys. Chem. 76 (1972) 3518.
[27] W. Wong, D.D. Davis, Int. J. Chem. Kinet. 1 (1974) 401.
[28] K.-J. Hsu, S.M. Anderson, J.L. Durant, F. Kaufman, J. Phys. Chem. 93 (1989) 1018.